Aerosol Science 40 (2009) 29 – 43

Contents lists available at ScienceDirect

Aerosol Science

journal homepage: www.elsevier.com/locate/jaerosci

Modeling of ultrafine particle dispersion in indoor environments with an improved drift flux model

Bin Zhao[a,*], Chun Chen[a], Zhongchao Tan[b]

[a]Department of Building Science, School of Architecture, Tsinghua University, Beijing 100084, China
[b]Department of Mechanical and Manufacturing Engineering, Schulich School of Engineering, University of Calgary, Alberta, Canada

ARTICLE INFO

Article history:
Received 19 March 2008
Received in revised form
24 July 2008
Accepted 5 September 2008

Keywords:
Indoor air quality (IAQ)
Ultrafine particle
Dispersion/distribution
Drift flux model
Computational fluid dynamics

ABSTRACT

Ultrafine particle (sub-100 nm in diameter) can transport toxic chemicals into the human respiratory system, causing more damage to macrophage phagocytosis than micron particles do. Therefore, various computational fluid dynamics (CFD) models have been developed to help understand the transport and dispersion of these particles in indoor environments. This study is focused on an improved drift flux model that incorporates not only the effect of gravitational settling but also other mechanisms. After an experimental validation of the improved model, it was used to analyze the dispersion of different sizes of ultrafine particles in two typical types of indoor environments (mixing and displacement ventilation). It was found that mixing ventilation had higher concentrations of ultrafine particles than displacement ventilation in the zone below 1 meter, and this finding is different from micron range particles. In addition, both ventilation modes were insensitive to the particles in the range of 0.01–0.1 μm in diameter.

1. Introduction

Epidemiologic evidence has shown a strong association between exposure to airborne particles and adverse health effects, including aggravation of respiratory and cardiovascular diseases, lung diseases, decreased lung function, asthma attacks, heart attacks and cardiac arrhythmia (EPA, 2005). Ultrafine particles (sub-100 nm in diameter) can transport toxic chemicals into the human respiratory system and damage macrophage phagocytosis more than micron particles do, implying a greater threat to human health. There is also evidence that some particles that are non-toxic in the micron size range may be toxic in the nano range. Studies using rats exposed to 250 and 20 nm titanium oxide (TiO_2) particles of the same mass showed that more ultrafine (20 nm) particles were stored in the interstitial tissue of the lungs, which developed noticeable inflammatory responses (Ferin et al., 1990). This was also true with Teflon particles, which are normally considered an inert substance. Unassuming concentrations of 30 nm Teflon fume particles produced acute pulmonary toxicity in rats (Kittelson, 1998).

The reality that exposure to ultrafine particles causes adverse health effects has raised a significant research interest in simulating particle dispersion/distribution indoors. Accurate simulation of indoor particle dispersion/distribution is of great assistance to the understanding the indoor particle dispersion characteristics, assessing the human exposure to particle pollution and designing indoor environments.

Computational fluid dynamics (CFD) is one powerful approach to simulating particle dispersion indoors. CFD models can provide detailed spatial distributions of air pressure, velocity, temperature, humidity and contaminant concentration by simultaneously solving the conservation equations of mass, momentum, energy and species concentrations. For the purpose of

* Corresponding author. Tel.: +86 10 62779995; fax: +86 10 62773461.
E-mail address: binzhao@tsinghua.edu.cn (B. Zhao).

0021-8502/$ - see front matter © 2008 Elsevier Ltd. All rights reserved.
doi:10.1016/j.jaerosci.2008.09.001

Nomenclature

C (mg/m^3)	the averaged concentration of particles
C_{in} (mg/m^3)	the particle concentration at inlet of ventilation room
C_{out} (mg/m^3)	the particle concentration at outlet of ventilation room
C_c	the Cunningham coefficient caused by slippage
C_s	a constant
C_t	a constant
C_m	a constant
C^*	the normalized particle concentration
D (mg/s)	the drift flux caused by the momentum change rate per unit volume of particle phase
d_p (m)	the particle diameter
$\sum F_j$ (m/s^2)	the total forces exerted on the particles per unit mass
F_{th} (mg/s)	the drift flux caused by the thermal force on particles
F_{thj} (m/s^2)	the thermal force in j direction
G (mg/s)	the drift flux caused by gravity
g_j (m/s^2)	the acceleration of gravity in j direction
Kn	the Knudsen number
k_p (W/(m K))	the thermal conductivity of the particle
m_p (mg)	the mass of a particle
R (m^2/(s^2 K))	the ideal gas constant
S_C (kg/(m^3 s))	the generating rate of the particle source
S_{mj} (kg/(m^2 s^2))	the momentum source of particles in j direction
S_{mp} (mg/s)	the drift flux caused by the particle fluctuation due to turbulence
T (K)	the absolute temperature
T_{in} (°C)	the air temperature at inlet of ventilation room, or the inlet of ducts
T_{out} (°C)	the air temperature at outlet of ventilation room, or the outlet of ducts
t (°C)	the air temperature
V_j (m/s)	the averaged fluid (air) velocity in j direction
V_{sj} (m/s)	the gravitational settling velocity of particles in j direction
V_{pj} (m/s)	the averaged particle velocity in j direction
V_{pi} (m/s)	the averaged particle velocity in i direction
$V_{slip,j}$ (m/s)	the slippage velocity of a particle with respect to air
τ_p (s)	the particle relaxation time
μ (N s/m^2)	the molecular dynamic viscosity of air
ρ_p (kg/m^3)	the particle density
λ (m)	the mean free length of the air molecule
υ_t (m^2/s)	the turbulent kinetic viscosity
Θ	the normalized temperature
σ_C	the turbulent Schmidt number of C
ε_p (m^2/s)	the particle eddy diffusivity

simulating indoor particle concentration accurately and quickly, the Eulerian methods, which solve the particle mass/number concentration conservation equation based on the assumption of treating the particles as a continuum, are widely used.

Among the Eulerian methods for particle dispersion simulation in indoor environments, the drift flux model is considered acceptable as it considers the slippage between particle phase and fluid (air) phase. It takes the effect of the "drift flux", due to the gravitational settling, into consideration for the analysis of the continuity (or conservation of mass of particles). This is referred to as the drift flux model:

$$\frac{\partial[(V_j + V_{sj})C]}{\partial x_j} = \frac{\partial}{\partial x_j}\left(\frac{\upsilon_t}{\sigma_C}\frac{\partial C}{\partial x_j}\right) + S_C \tag{1}$$

where V_j and V_{sj} are the averaged fluid (air) velocity and the gravitational settling velocity of particles in j direction, respectively, C is the averaged concentration of particles (mass or number per unit volume), σ_C is the turbulent Schmidt number of C, which is usually equal to 1.0 (Holmberg & Li, 1998; Murakami, Kato, Nagano, & Tanaka, 1992), S_C is the generating rate of the particle source and υ_t is the turbulent kinetic viscosity. The drift flux model described in Eq. (1) is an improvement of the traditional transport model of gas contaminant (passive scalar) concentration by adding the drift flux term, $\partial(V_{sj}C)/\partial x_j$, into the equation.

This particle drift flux is the result of transport of particles due to the velocity difference between the particles and the air. It is caused by particle drag force and gravity, which are dominant for bigger particles with higher inertia.

The drift flux model has been employed for indoor particle dispersion simulation by different researchers (Chen, Yu, & Lai, 2006; Gao & Niu, 2007; Holmberg & Chen, 2003; Holmberg & Li, 1998; Murakami et al., 1992; Zhao, Li, & Zhang, 2004). These studies concluded that fine particles dispersed like gas species and that they traveled with the indoor air without any slippage due to their relatively small settling velocities. For instance, Murakami et al. (1992) suggested that particles smaller than 4.5 μm could be treated as passive scalar (gas contaminant), while Liu and Zhai (2007) proposed that the slippage of sub-20 μm particles could be neglected.

However, gravitational settling is not the only mechanism that causes particle slippage. Thermophoresis and turbulence can also cause the slippage of particles in air. Thermophoresis may play an important role on the motion of ultrafine particles for non-isothermal cases, where the temperature varies indoors. Furthermore, the dispersion of ultrafine particles is also influenced by turbulence, which is referred to as another type of drift flux. In modeling the dispersion of ultrafine particles, it has not been clear whether these effects can be ignored or not.

The main objective of this paper is to develop a generalized drift flux model to quantify the effects of various factors that may contribute to the drift flux. The question to be answered is which factors can be ignored for ultrafine particle dispersion modeling. The mass and momentum conversation equations of gas–particle two-fluid mixture are employed to deduce the generalized drift flux model. This model is validated by laboratory experiments, where spatial distributions of concentrations of ultrafine particles, air velocity and temperature are measured in a non-isothermal chamber. The improved model is then employed to study the dispersion of ultrafine particles in two typical indoor environments (mixing and displacement ventilation). Although previous studies (Zhao, Li, et al.,2004; Zhao, Zhang, Li, Yang, & Huang, 2004) have tried to numerically analyze the particle dispersion in two similar cases by both Eulerian and Lagrangian models, there are no results for ultrafine particles, and most importantly, there is no analysis of the different effects causing particle slippage to air phase.

2. Model development

The key point of the drift flux model is the consideration of the drift flux effect caused by the slippage between the particles and the air. Mathematically, it is necessary to add a drift flux term into the mass/number conservation equation. With this approach, a modeler needs to solve only the particle mass/number (particle concentration) conservation equation to get the particle concentration at a minimum computational cost. In this study, the generalized drift flux model is developed based on the conservations of mass and momentum of particle phase in a gas–particle mixture. The steady, averaged mass conservation equation and momentum conservation equation in j direction of the particle phase are as follows (Zhou, 1993):

$$\frac{\partial(V_{\mathrm{p}j}C)}{\partial x_j} = \frac{\partial}{\partial x_j}\left[\varepsilon_{\mathrm{p}}\frac{\partial C}{\partial x_j}\right] + S_C \tag{2}$$

$$\frac{\partial(V_{\mathrm{p}j}V_{\mathrm{p}i}C)}{\partial x_i} = \frac{C(V_{\mathrm{p}j}-V_j)}{\tau_{\mathrm{p}}} + Cg_j + C\sum F_j + S_{\mathrm{m}j} \tag{3a}$$

$$S_{\mathrm{m}j} = \frac{\partial}{\partial x_i}\left[\varepsilon_{\mathrm{p}}C\left(\frac{\partial V_{\mathrm{p}j}}{\partial x_i}+\frac{\partial V_{\mathrm{p}i}}{\partial x_j}\right)\right] + \frac{\partial}{\partial x_i}\left[\varepsilon_{\mathrm{p}}\left(V_{\mathrm{p}i}\frac{\partial C}{\partial x_j}+V_{\mathrm{p}j}\frac{\partial C}{\partial x_i}\right)\right] \tag{3b}$$

$$\tau_{\mathrm{p}} = \frac{C_{\mathrm{c}}\rho_{\mathrm{p}}d_{\mathrm{p}}^2}{18\mu} \tag{3c}$$

where $V_{\mathrm{p}j}$ and $V_{\mathrm{p}i}$ are the averaged particle velocities in j and i directions, respectively, ε_{p} is the particle eddy diffusivity, τ_{p} is the particle relaxation time that is calculated by Eq. (3c), $\sum F_j$ are the total forces exerted on the particles, g_j is the acceleration of gravity in j direction, $S_{\mathrm{m}j}$ is the momentum source of the particles in j direction, μ is the molecular dynamic viscosity of air, ρ_{p} and d_{p} are the particle density and diameter, respectively, and C_{c} is the Cunningham coefficient caused by slippage. For sub-100 nm particles, C_{c} can be calculated by (Hinds, 1999):

$$C_{\mathrm{c}} = 1 + \frac{\lambda}{d_{\mathrm{p}}}\left(2.514 + 0.8\times\exp\left(-0.55\frac{d_{\mathrm{p}}}{\lambda}\right)\right) \tag{4}$$

where λ is the mean free path of the air molecules and d_{p} is the particle diameter.

The left hand side (lhs) of the momentum equation (Eq. (3a)) is the momentum change rate per unit volume of particle phase; the first term of the right hand side (rhs) in Eq. (3a) is the drag force due to the difference between the velocities of particle and fluid; the second term of the rhs is the gravity in j direction; the third term of the rhs represents other forces on the particles in j direction, which may include virtual mass force, basset force, pressure force, thermal force, etc. The last term of the rhs is the momentum transport by particle fluctuation due to turbulence, as described using Eq. (3b).

The first and second terms of the rhs in Eq. (3b) represent the correlation of particle turbulent fluctuation velocities and that of particle fluctuation velocity and concentration, respectively. Here, the slippage velocity of particle between air ($V_{\mathrm{slip},j}$) is defined as the difference between the averaged particle velocity ($V_{\mathrm{p}j}$) and the averaged air velocity (V_j):

$$V_{\mathrm{slip},j} = V_{\mathrm{p}j} - V_j \tag{5}$$

Rewriting Eq. (3a) gives

$$V_{\mathrm{slip},j} = \tau_{\mathrm{p}} g_j + \tau_{\mathrm{p}} \sum F_j + \frac{\tau_{\mathrm{p}}}{C} S_{\mathrm{m}j} - \frac{\tau_{\mathrm{p}}}{C} \frac{\partial (V_{\mathrm{p}j} V_{\mathrm{p}i} C)}{\partial x_i} \tag{6}$$

Substituting Eq. (5) into Eq. (2), one can get

$$\frac{\partial [(V_j + V_{\mathrm{slip},j})C]}{\partial x_j} = \frac{\partial}{\partial x_j}\left[\varepsilon_{\mathrm{p}} \frac{\partial C}{\partial x_j}\right] + S_C \tag{7}$$

This is the generalized drift flux model that incorporates all the effects causing "drift" of particles. Referring to Eq. (6), the slippage velocity of particles is defined by gravity, thermal force by thermophoresis effect, particle fluctuation due to turbulence and particle acceleration. For the fine particles in indoor environments, the particle eddy diffusivity can be simplified as 1 (Hinze, 1975; Zhou, 1993). If the gravitational settling velocity is treated as the only slippage velocity of particles, that is, keeping only the first term in Eq. (6), the generalized drift flux model returns to the traditional one as described using Eq. (1).

The generalized drift flux model equation (Eq. (6)) is used to calculate the slippage velocity of particles. In the analysis above, other forces acting on the ultrafine particles were neglected, because they are one or several orders smaller than gravity (Zhao, Zhang, et al. 2004), i.e. Basset force, virtual mass force caused by unsteady flow and pressure gradient force. The lift force may only be dominant very near the walls due to the large velocity gradient there. Therefore, herein only thermal force is considered for non-isothermal cases studied.

The second term of the rhs of Eq. (6) is the thermal force and can be calculated by (Talbot, Cheng, & Schefer, 1980)

$$F_{\mathrm{th}j} = -\frac{6\pi d_{\mathrm{p}} \mu^2 C_{\mathrm{s}} (K + Kn)}{\rho (1 + 3C_{\mathrm{m}} Kn)(1 + 2K + 2C_{\mathrm{t}} Kn)} \frac{1}{m_{\mathrm{p}} T} \frac{\partial T}{\partial x_j} \tag{8a}$$

$$K = \frac{15\mu R}{4k_{\mathrm{p}}} \tag{8b}$$

where $C_{\mathrm{s}} = 1.17$, $C_{\mathrm{t}} = 2.18$, $C_{\mathrm{m}} = 1.14$, Kn is the Knudsen number and $Kn = 2\lambda/d_{\mathrm{p}}$. m_{p} is mass of particle, T is the absolute temperature of particle, k_{p} is the thermal conductivity of the particle and R is the ideal gas constant.

The third term of the rhs of Eq. (6) stands for the velocity difference caused by velocity and mass transport due to particle turbulence, and the fourth term represents the velocity difference by particle acceleration. For ultrafine particles, they are modeled by the results of air phase. Thus, these two terms can be calculated as

$$\frac{\tau_{\mathrm{p}}}{C} S_{\mathrm{m}j} = \frac{\tau_{\mathrm{p}}}{C} \frac{\partial}{\partial x_i}\left[\varepsilon_{\mathrm{p}} C \left(\frac{\partial V_j}{\partial x_i} + \frac{\partial V_i}{\partial x_j}\right)\right] + \frac{\partial}{\partial x_i}\left[\varepsilon_{\mathrm{p}} \left(V_i \frac{\partial C}{\partial x_j} + V_j \frac{\partial C}{\partial x_i}\right)\right] \tag{9}$$

$$\frac{\tau_{\mathrm{p}}}{C} \frac{\partial (V_{\mathrm{p}j} V_{\mathrm{p}i} C)}{\partial x_i} = \frac{\tau_{\mathrm{p}}}{C} \frac{\partial (V_j V_i C)}{\partial x_i} \tag{10}$$

After solving the mass, momentum and energy conservation equations of fluid (air) phase, the slippage velocity can be calculated with Eqs. (6), (8), (9) and (10), and the particle dispersion/distribution can be calculated with Eq. (7).

Note that the effect of particles on turbulence is not considered in the above analysis, because it is believed that the low particle loadings have only a very small effect when compared to the high turbulence levels of indoor air. As the volume fraction of particles in a typical indoor environment is in the order of 10^{-10}, it obeys the one-way coupling rule (Elghobashi, 1994). In addition, the particle distribution may be simulated based on the converged air velocity field without interaction on air velocity (Zhao, Li, et al., 2004). Thus, we can solve the fluid (air) phase equations following the same procedure as that for one phase simulation for particle concentration distribution using Eqs. (6)–(10). The simulation of air phase follows the model and algorithm employed by Zhao, Li, and Yan (2003); and the particle deposition to wall surfaces is treated as additional boundary conditions when calculating the improved drift flux model, which follows the method proposed by Zhao, Li, et al. (2004).

3. Validation of the model using laboratory experiment

3.1. Experimental setup

The improved model for ultrafine particle dispersion simulation was validated for a non-isothermal case using a simulated room with dimensions of 33″ wide×33″ high × 62″ long, as shown in Fig. 1. Two tape heaters (720 and 360 W) were employed to

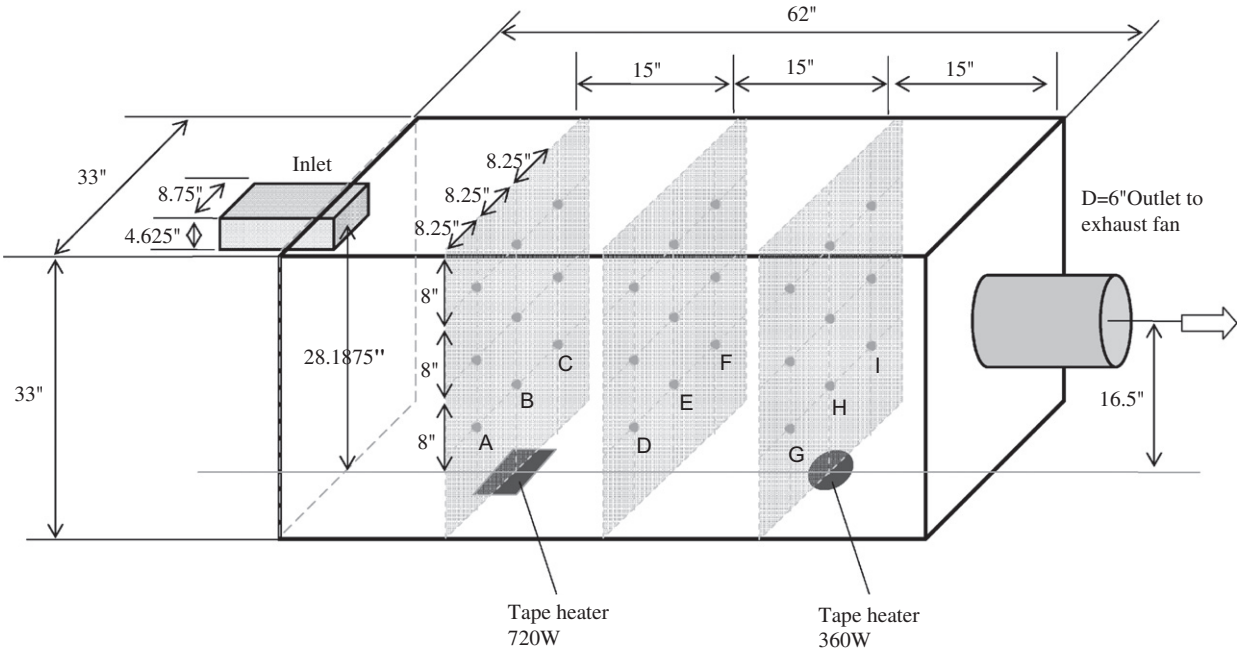

Fig. 1. The simulated ventilated chamber and the corresponding sampling points.

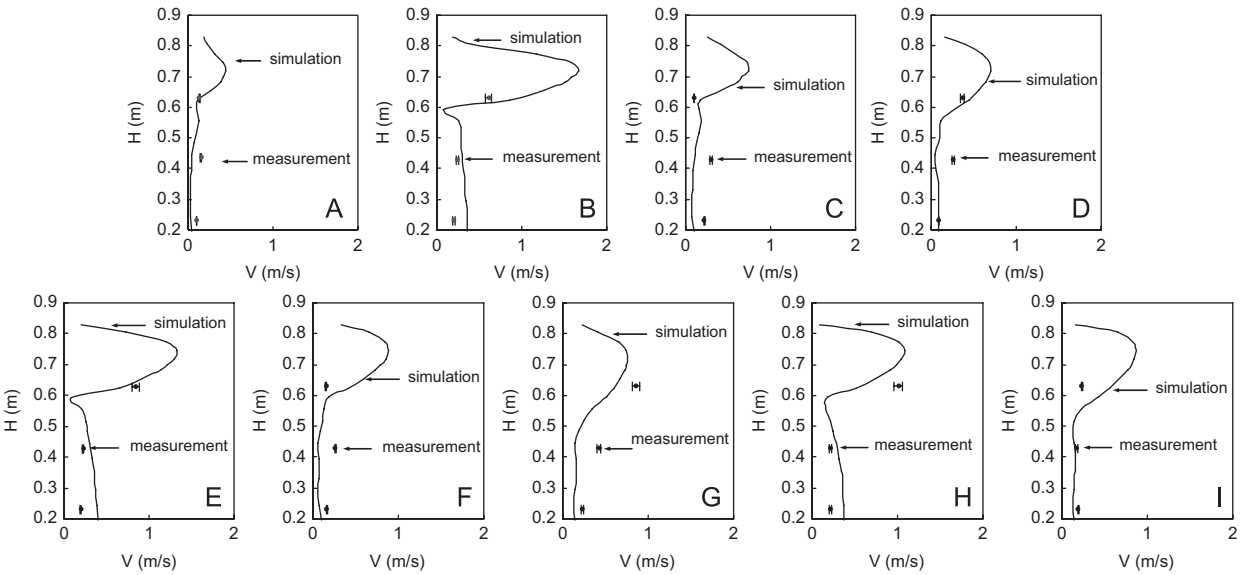

Fig. 2. Comparison of measured velocity with the calculated data.

simulate the heating sources, as well as ultrafine particle sources on the floor. Air was pulled through the chamber by a centrifugal fan controlled by a variable frequency driver (VFD). Air velocity, temperature and particle concentrations were measured at inlet, outlet and 27 locations (3×9 points) within the airspace (see Fig. 1).

The velocity and temperature distributions were measured simultaneously by using a hotwire anemometer (VelociCalc® air velocity meter, Model 9515, TSI Inc.). According to the manufacture, the accuracy of velocity measurement is 5% of the reading or 0.01 m/s, whichever is greater, and that of the temperature measurement is 0.3 °C of the reading or 0.1 °C, whichever is greater. The measured temperature difference between the inlet and outlet was about 10 °C, which is close to the actual case in a typical ventilated indoor environment.

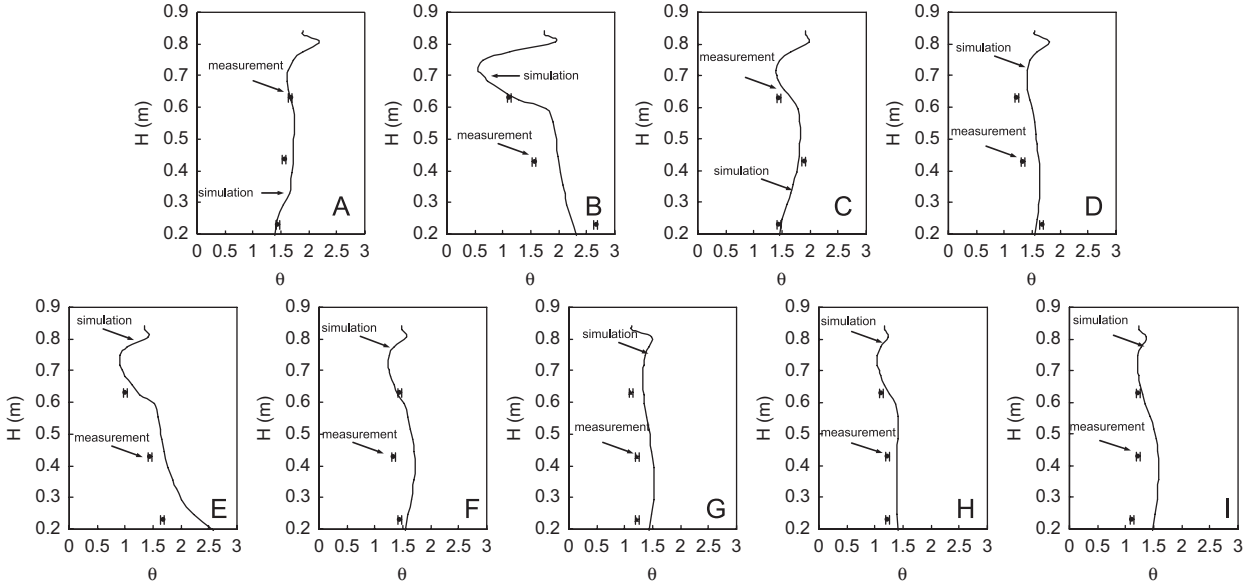

Fig. 3. Comparison of the measured temperature with the calculated data.

The particle concentrations were measured using a scanning mobility particle sizer (TSI SMPS 3936). For all the measurements herein each scan took 135 s for particles in the range of 5.84–224.7 nm. Three replications were taken for each data point. The sampling flow rate was set to be 1 l/min. Results were pre-set to automatically export with a unit of dw/dlogDp (number/cm^3) into a computer for future data analysis.

The sources of the particles were characterized before measuring particle concentrations at the 27 points. Ultrafine particles (NaCl) were injected using a 1/4″ tube into the room at the rectangular inlet that was located in the top left of the chamber. The particles fed to the inlet were generated using a collision-type atomizer (TSI model 3076) using a NaCl solution mixed with deionized water with a concentration of 0.1 g/l. The atomizer was claimed to have a stable output, and it was also calibrated and confirmed in our laboratory (Golshahi, 2007) shortly prior to our study herein. In addition to the particles fed at the inlet from the atomizer, those generated by the heating tapes on the floor were also characterized and their outputs were confirmed to be stable.

3.2. Model validation

Figs. 2 and 3 show the comparison of the calculated and measured velocities and temperatures, respectively, at the 27 points within the airspace. In Fig. 3, the x-axis is the normalized temperature, which is defined by $\theta = (T - T_{in})/(T_{out} - T_{in})$, where T_{in} and T_{out} are the inlet and outlet temperatures, respectively. The error bars are calculated from the accuracy of the instrument as introduced in Section 3.1. Both Figs. 2 and 3 show that the predicted air velocity and temperature profiles match the measurements well. These correctly calculated air phase parameters ensure the correct prediction of ultrafine particle distribution.

Fig. 4 shows the comparison of the calculated ultrafine particle concentration with the measurements for particles with diameters of 10.2, 49.6 and 101.8 nm. Similar to Fig. 3, the normalized concentration, $C^* = C/C_{in}$, is used on the x-axis in Fig. 4, where C_{in} stands for the inlet particle concentration. The error bars are the standard deviations of the corresponding three replications. The small error bars indicated that the measurements were consistent and the variability was small. The predicted concentration profiles match the measurements very well. The differences between the model and the experiments may have resulted from errors introduced in particle concentration measurements. Overall, the averaged relative difference of calculations between measurements was below 10%. Thus, the improved drift flux model was validated well by the comparison of the calculated data with the measurements.

4. Simulation of ultrafine particle distribution in two typical indoor environments

4.1. Case description

Two field measurements from the mixing and displacement ventilation cases are compared with the modeling results using the model introduced herein. These two cases are typical ventilation modes adopted for actual office buildings. The experiments

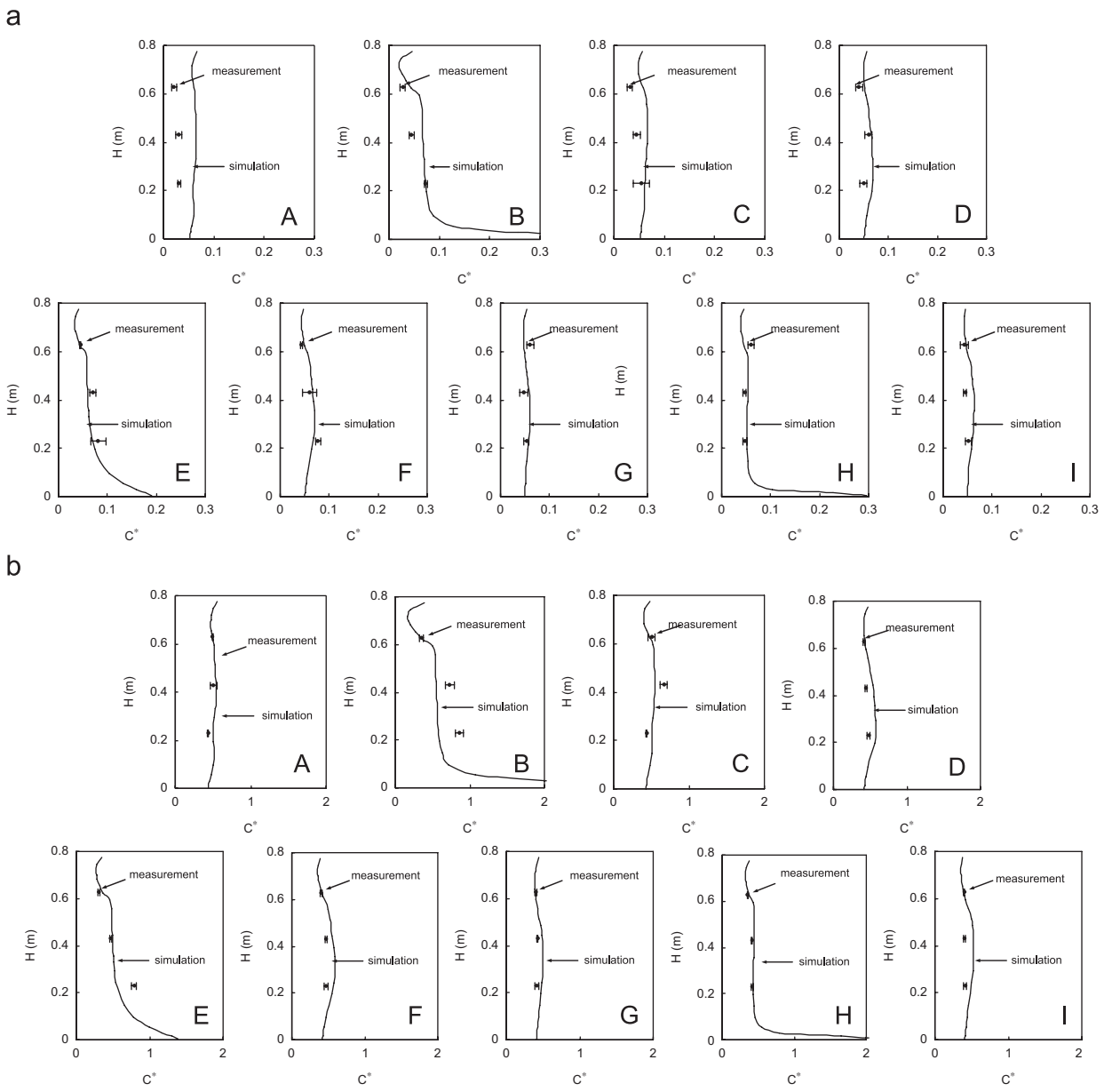

Fig. 4. Comparison of the measured concentration with the calculated data: (a) diameter, 0.0102 μm, (b) diameter, 0.0496 μm, and (c) diameter, 0.1018 μm.

were conducted using a full-scale environmental chamber (5.16×3.65×2.44 m) as shown in Fig. 5 (He, 2003). Two different air distribution systems were studied using displacement and grille diffusers. The displacement diffuser was located on the floor against the west wall, and the ceiling exhaust was the outlet for the displacement ventilation. In the other ventilation mode, the exhaust at the lower level (object 4) was coupled with the grille diffuser at the higher level (object 2). Fig. 6 shows the sketch of the room and the positions for eight measuring poles (He, 2003). Heat sources, including human simulators, lights, and computers, are present in the real office, as well as in the simulations. Particle sources are the human simulators. For simplification, the generating rates of different sizes of particles are assumed to be the same. Table 1 summarizes the parameters of the supply and return air including inlet temperature, outlet temperature, inlet velocity and outlet velocity.

The comparisons of the model predictions and the experimental measurements by He (2003) are also presented to confirm that the modeling results of velocity and temperature are correct. According to He (2003), 28 hot-sphere anemometers were used to measure the temperature and velocity distributions in the room. The anemometers could measure velocities in the range of

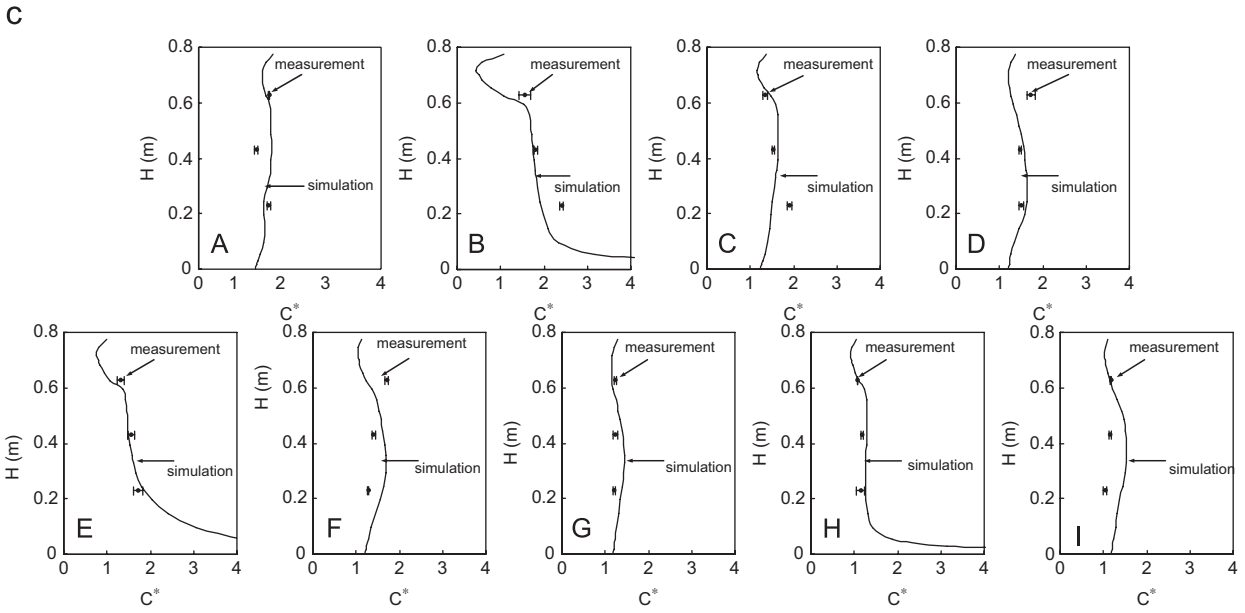

Fig. 4. (*continued*).

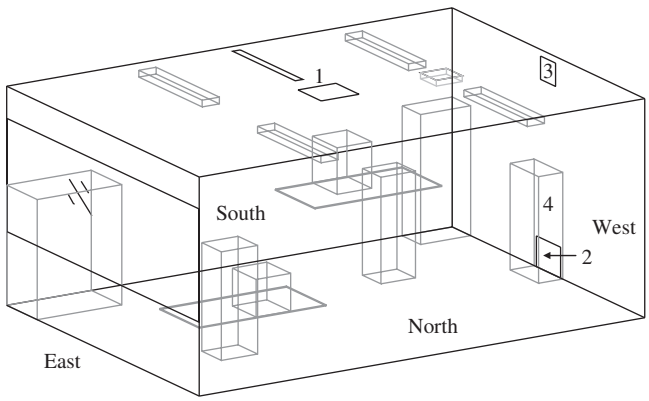

Fig. 5. Room configuration and ventilation systems (He, 2003): 1—ceiling outlet (for displacement case), 2—outlet (for missing case), 3—grille diffuser, and 4—displacement diffuser.

Table 1
Supply and return parameters.

	Displacement case	Grille case
Inlet temperature (°C)	15.88	18.49
Outlet temperature (°C)	24.80	24.16
Inlet velocity (m/s)	0.3	1.55
Outlet velocity (m/s)	0.29	0.47
Ventilation rate (m^3/s)/ACH	0.0562/4.1	0.0674/5.3

0.05–5 m/s with an accuracy of 0.01 m/s or ± 2% of the reading when velocity was above 0.15 m/s. However, the measurements were not reliably when the velocity was below 0.10 m/s. The hot-sphere anemometer measured temperatures at a resolution of 0.3 °C. For either ventilation system, the measurements were conducted twice under steady-state conditions. Before each test, the room was ventilated for more than 12 h to reach a steady thermal state.

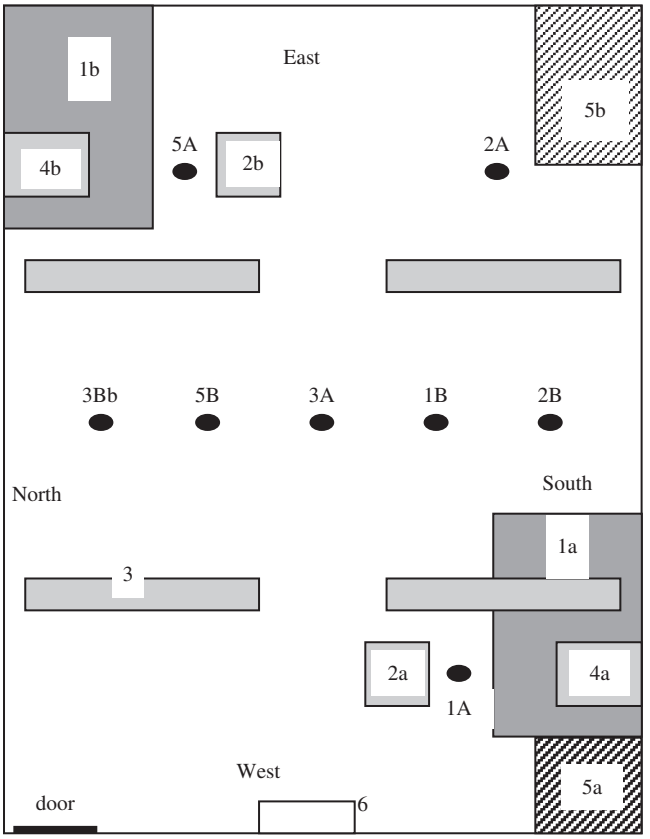

Fig. 6. Sketch of the room and positions for eight measuring poles: 1A, 2A, 3A, 5A and 1B, 2B, 3B, 5B (He, 2003): 1—table (a, b), 2—human simulators (a, b), 3—lights, 4—computers (a, b), 5—cabinets (a, b), and 6—displacement diffuser.

4.2. Results and discussion

4.2.1. Ultrafine particle concentration distribution

Figs. 7–11 show the comparison of the calculated values and the measured data of velocity and temperature at eight poles shown in Fig. 6, where Figs. 7 and 8 present the displacement case and Figs. 10 and 11 illustrate the mixing one. The error bars are calculated from the accuracy of the instrument as introduced in Section 4.1. The graphs show that the predicted velocity and temperature profiles match the measurements well (averaged relative difference of calculations between measurements was below 8%) for the two cases.

Figs. 9 and 12 show the results of the concentration distributions of particles with different diameters, calculated using the improved drift flux model for the two cases, and the results of the concentration distributions calculated by the gas species conservation model are also compatible with the results calculated by the new model. The normalized concentration, C^*, is defined as $C^* = C/C_{\text{out}}$, as the supply particle concentration is assumed to be zero. This is reasonable to check the particle removal performance of the ventilation mode as being done in several previous studies (Gao & Niu, 2007; Zhao, Li, et al., 2004; Zhao, Zhang, et al., 2004). Fig. 13 shows the comparison of the ultrafine particle concentration distributions in the two different ventilation cases.

It should be highlighted that the concentration of 5-μm particles is higher than those of ultrafine particles for displacement case. The indoor particle concentration is determined by both deposited and exhausted mass. There are more 5-μm particles deposited due to the dominant effect of gravitational settling for the two cases. However, the displacement ventilation mode has a similar piston flow pattern (upward streams). This may make it easier for coarse particles to suspend indoors. Meanwhile, the fine particles may be easily exhausted. Generally, the total mass of exhausted and deposited ultrafine particles is greater than that of 5-μm particles. This leads to the lower concentrations of ultrafine particles in most locations. In the mixing case, the total mass of exhausted and deposited ultrafine particles is less than that of 5-μm particles, resulting the different distribution. This has been reported in previous publications using Lagrangian method (Zhao, Zhang, et al. 2004).

Previous studies of the distribution of particles with diameters greater than 5 μm showed that mixing ventilation had lower concentrations than displacement ventilation for different sizes of particles, and displacement ventilation was more sensitive to the particle size when considering gravitational sedimentation. However, ultrafine particle distribution differs significantly from

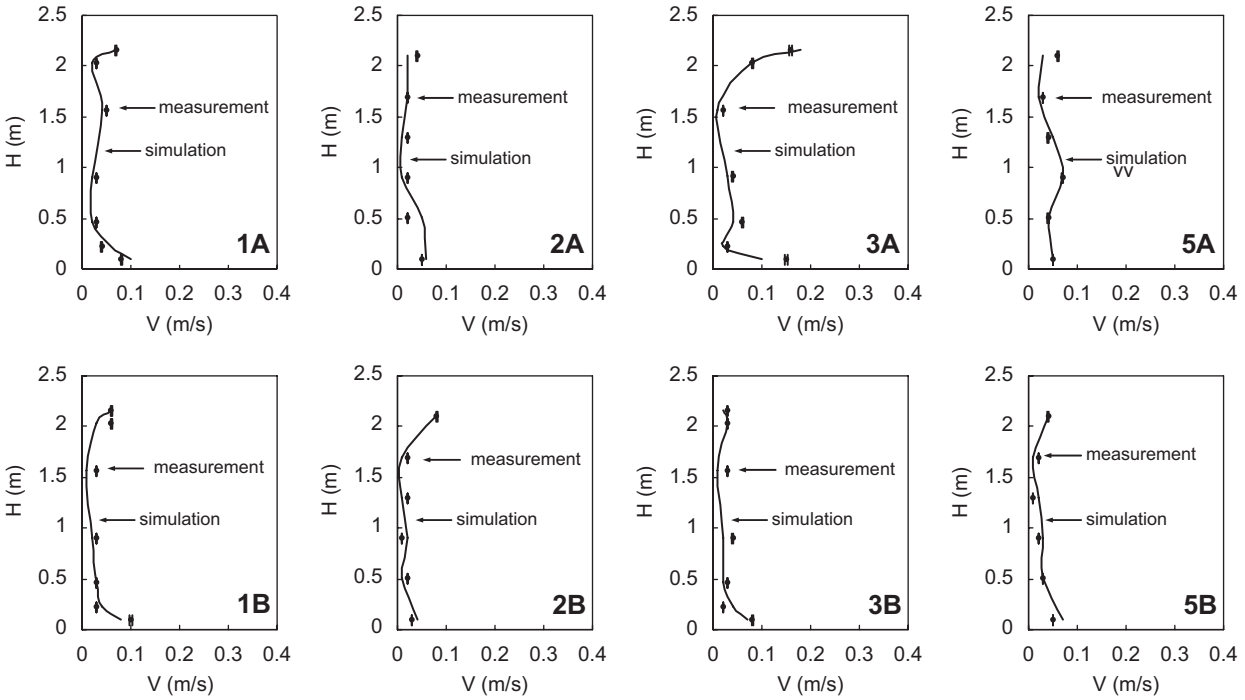

Fig. 7. Comparison of measured velocity distribution with the calculated data (displacement diffuser case).

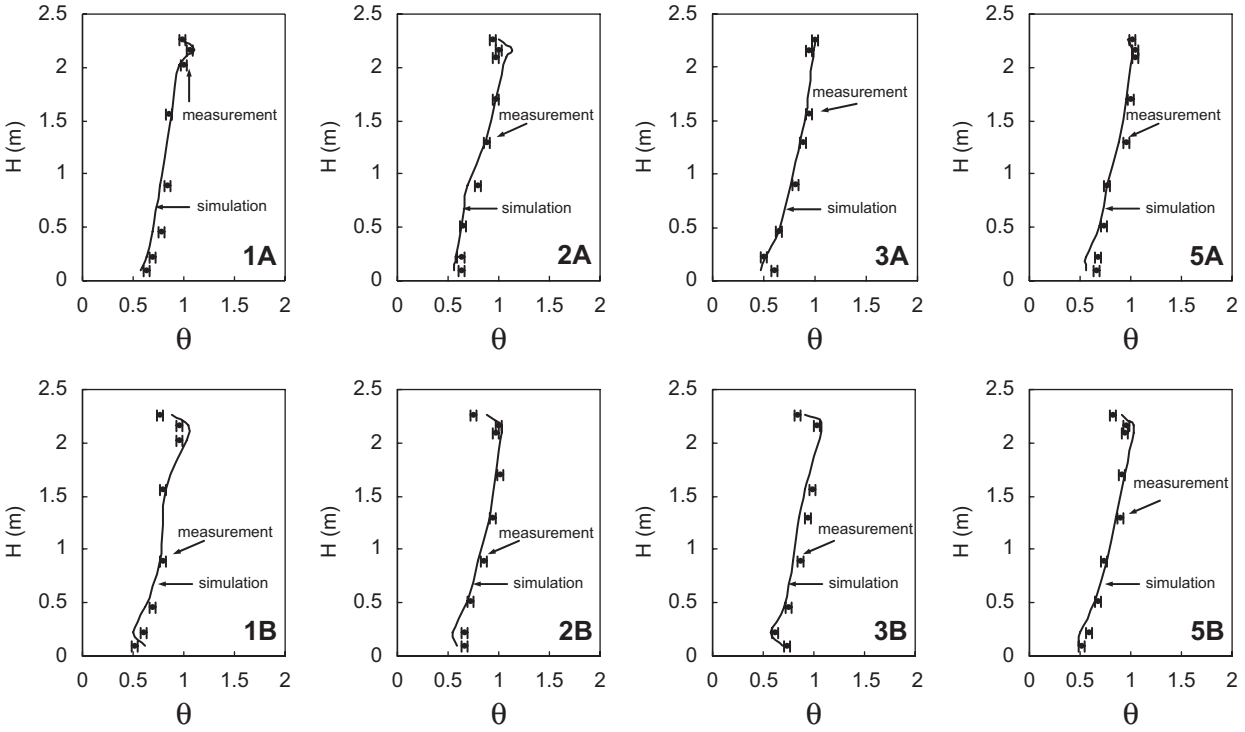

Fig. 8. Comparison of the measured temperature distribution with the calculated data (displacement diffuser case).

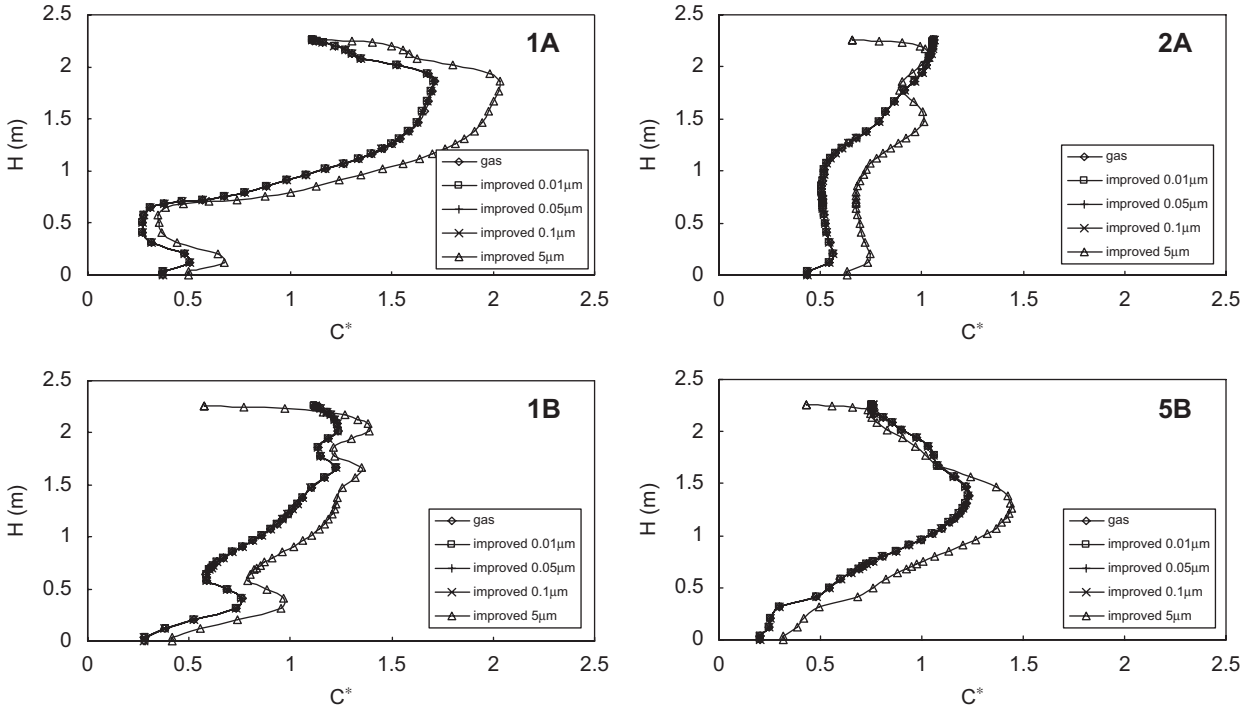

Fig. 9. Comparison of the concentration distribution calculated by different models (displacement diffuser case).

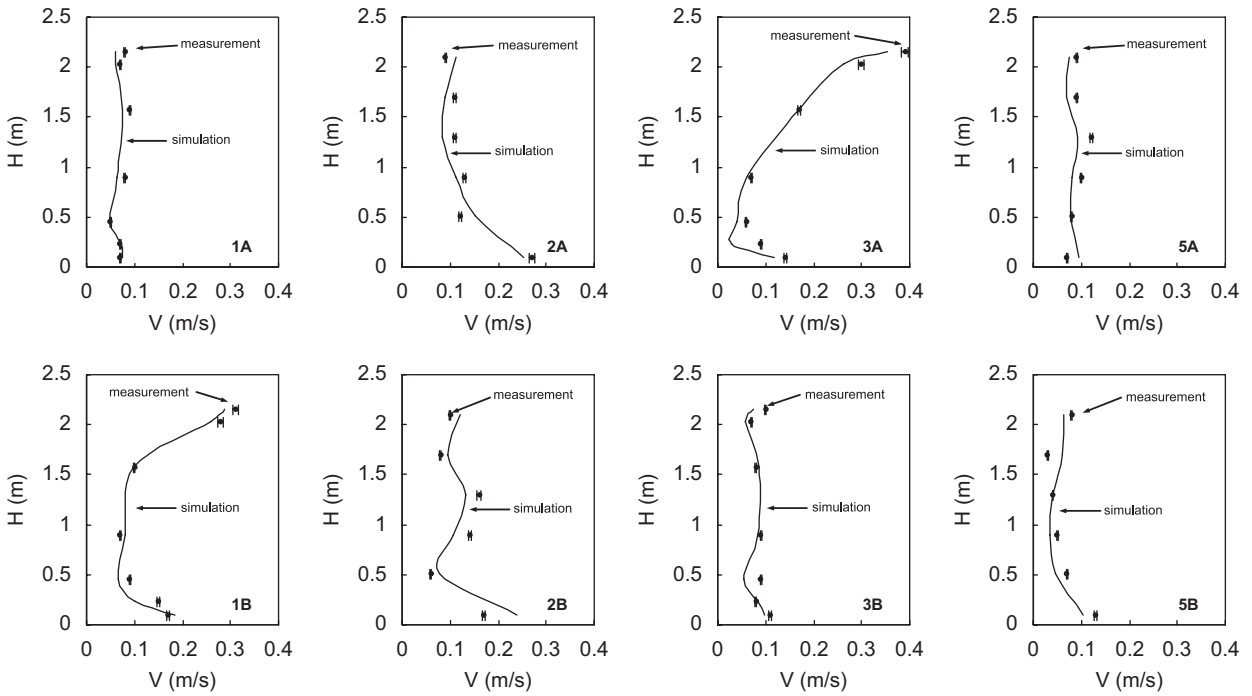

Fig. 10. Comparison of measured velocity distribution with the calculated data (Grille diffuser case).

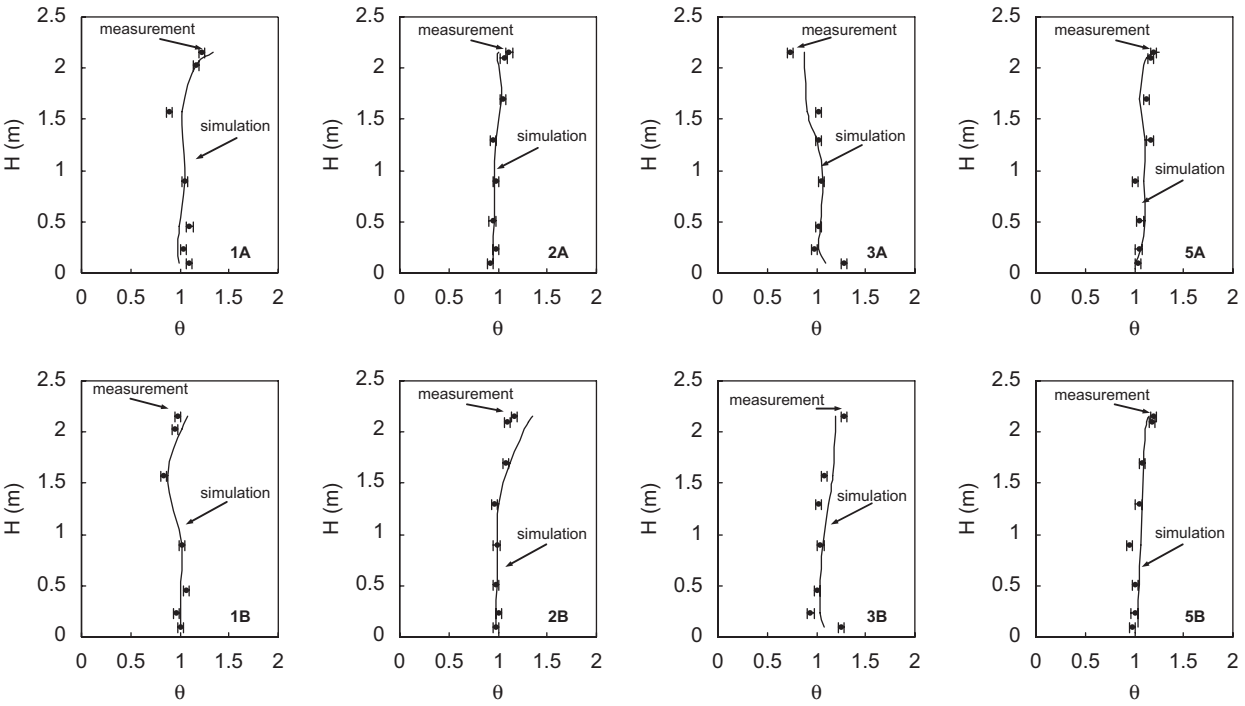

Fig. 11. Comparison of the measured temperature distribution with the calculated data (Grille diffuser case).

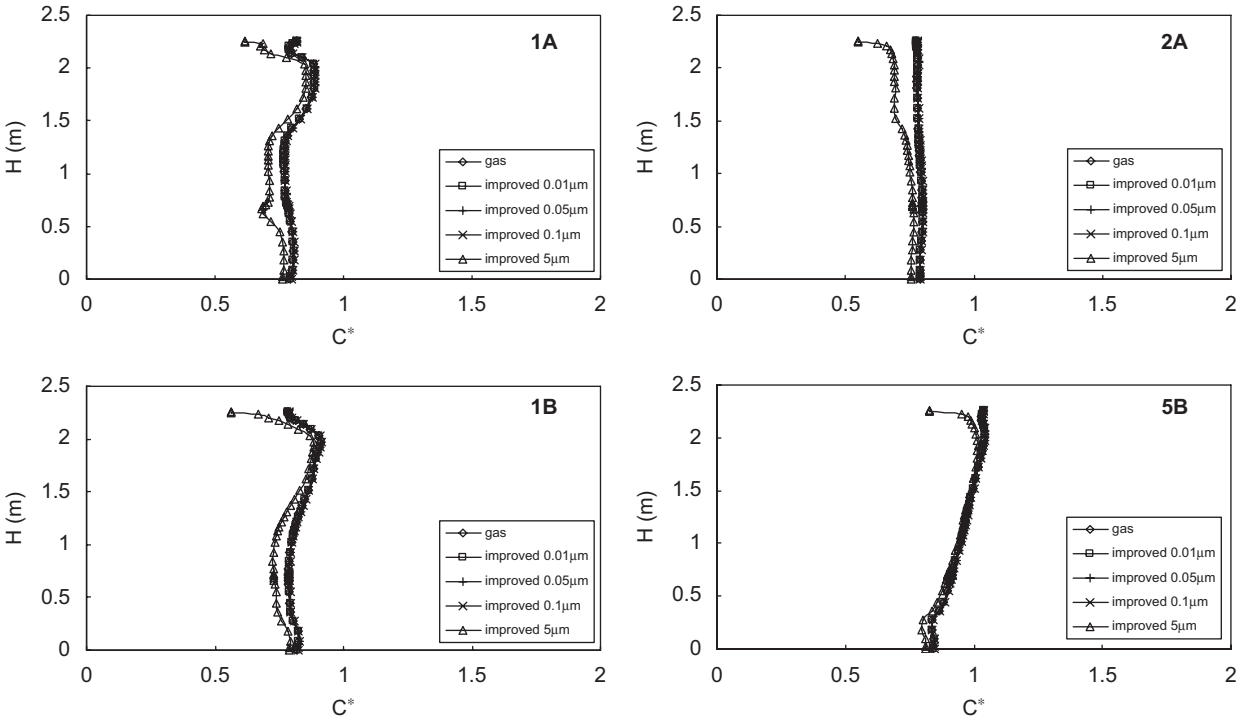

Fig. 12. Comparison of the concentration distribution calculated by different models (Grille diffuser case).

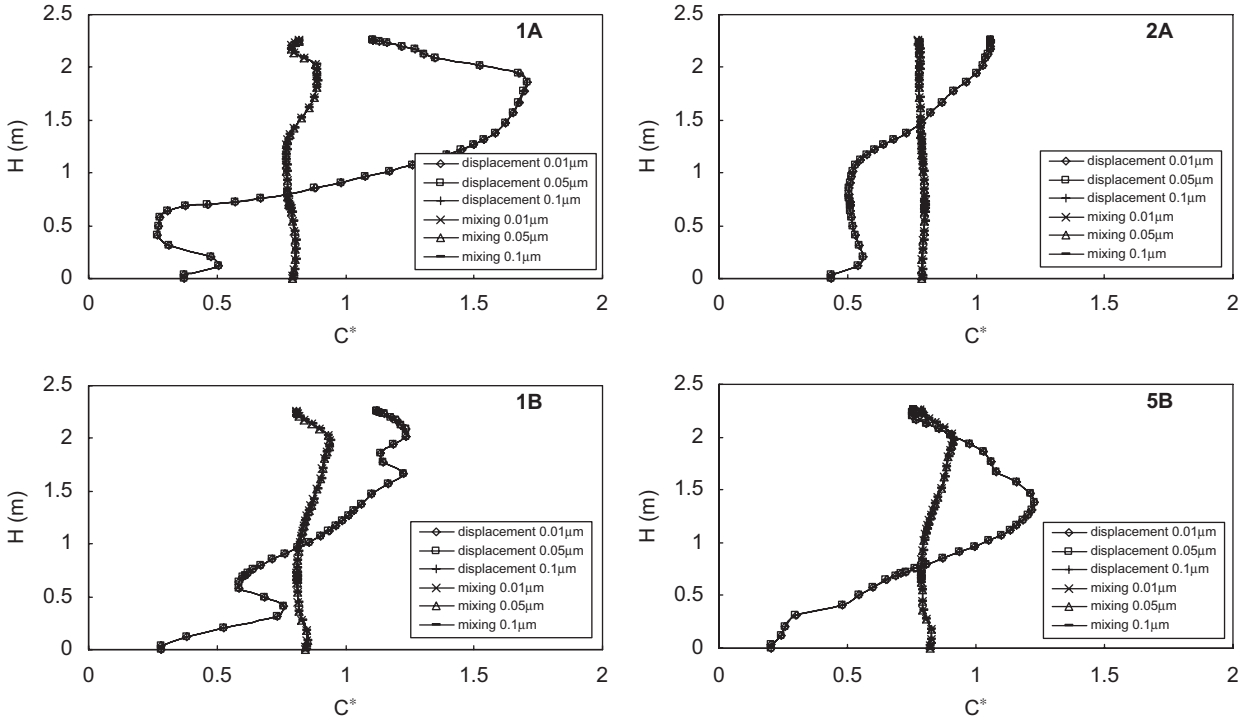

Fig. 13. Comparison of the ultrafine particle concentration distribution in the two different ventilation cases.

Table 2
Comparison of the effect of each force in displacement diffuser case.

d_p (μm)	G (mg/s)	F_{th} (mg/s)	D (mg/s)	S_{mp} (mg/s)
0.01	1.00E−10	1.00E−08	1.00E−12	1.00E−14
0.05	1.00E−09	1.00E−08	1.00E−11	1.00E−13
0.1	1.00E−08	1.00E−08	1.00E−10	1.00E−12
5	1.00E−05	1.00E−08	1.00E−07	1.00E−10

particulates with diameters greater than 5 μm. The results of ultrafine particle distribution show some important characteristics of ultrafine particle dispersion:

- Mixing ventilation has higher concentrations than displacement ventilation in some places, such as poles 2A, 1B and 5B, for ultrafine particles.
- Both ventilations are insensitive to the particle size when the diameter ranges from 0.01 to 0.1 μm.
- The concentration distributions of ultrafine particles in mixing ventilation are more symmetrical than the one in displacement ventilation.
- In the mixing ventilation case, the concentrations of ultrafine particles in the room are very close to the inlet concentration (the normalized concentration is in the range from 0.8 to 1).

In addition, both cases show that the results of the concentration distribution calculated by the two different models are almost the same when the diameter of particles is 0.01, 0.05 or 0.1 μm. But when the diameter of particle is 5 μm, the result is quite different. The reasons are discussed in the following section.

4.2.2. Analysis of the different effects on particle slippage

Tables 2 and 3 and Fig. 14 present the averaged orders of the effects causing particle slippage (Eq. (6)) for the two ventilation cases. For the sake of simplicity, the drift flux caused by the momentum change rate per unit volume of particle phase is expressed as D, the drift flux caused by the gravity is expressed as G, the drift flux caused by thermal force on particles is expressed as F_{th} and, the drift flux caused by the momentum transport by the particle fluctuation due to turbulence is expressed as S_{mp}. Figs. 9 and 12 indicate that the data simulated using the gas species conservation model and improved drift flux model are well

Table 3
Comparison of the effect of each force in grille diffuser case.

d_p (μm)	G (mg/s)	F_{th} (mg/s)	D (mg/s)	S_{mp} (mg/s)
0.01	1.00E−10	1.00E−08	1.00E−12	1.00E−14
0.05	1.00E−09	1.00E−08	1.00E−11	1.00E−13
0.1	1.00E−08	1.00E−08	1.00E−10	1.00E−11
5	1.00E−05	1.00E−08	1.00E−07	1.00E−08

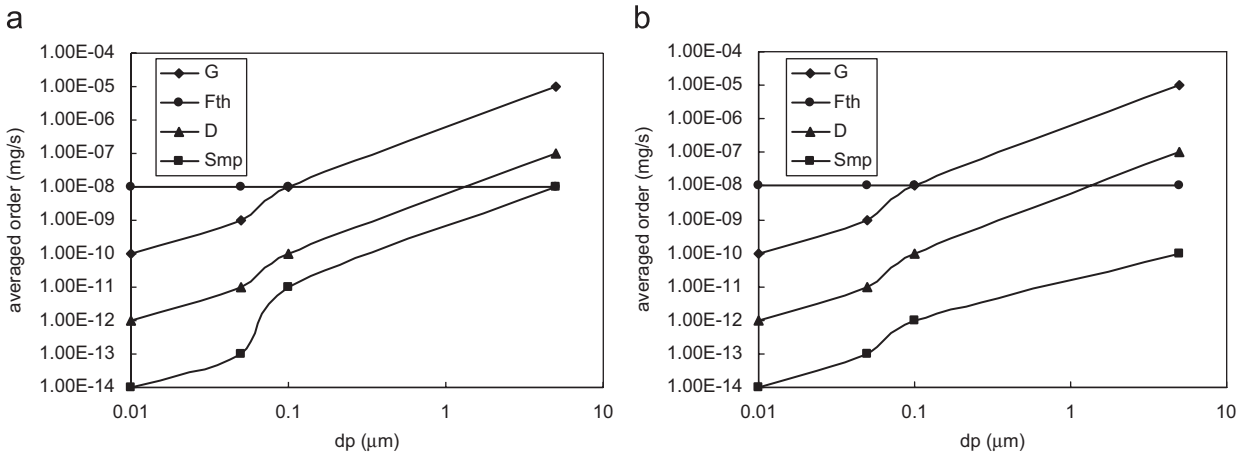

Fig. 14. Comparison of the effect of each force: (a) displacement diffuser case and (b) grille diffuser case.

matched for particulates with diameters of 0.01, 0.05 and 0.1 μm, but differ significantly for particulates with diameters of 5 μm. The explanations are as follows.

It can be seen from Tables 2 and 3 and Fig. 14 that D and S_{mp} are too small compared to the impact of gravitational sedimentation to affect the particle distribution in the room, so these factors can be neglected for a particle diameter in the range of 0.01–5 μm. For particles with a diameter greater than 5 μm, the effects of D and S_{mp} may be greater than that of the thermophoresis force. However, for ultrafine particles, the effects of D and S_{mp} become significant.

Regarding the effects of gravity and thermophoresis, gravitational sedimentation for particles with a diameter around 5 μm is far more prominent than the other three mechanisms. Therefore, the spatial distributions of these particles are very different from the situation of gas species. For particles with a diameter of around 0.1 μm, the effect of gravity is almost the same as that of the thermophoresis force; and, both driven forces are relatively small to affect the particle distribution. When the size of the particles gets smaller and smaller, the effect of thermophoresis force becomes stronger while the effect of gravity drops. For particles in the size range of 0.01–0.05 μm in diameter, the gravity is smaller than the thermophoresis force, but both forces are still too small to have a major impact on the particle dispersion.

5. Conclusions

In this paper, an improved drift flux model was introduced to simulate the dispersion of particles indoors. This study was focused on the particles with diameters of less than 0.1 μm, which are common in indoor environments. In this model, the mechanisms, including gravitational sedimentation, thermophoresis and turbulent transport, which are the most important factors of indoor particle distribution, were taken into consideration, in addition to the mechanisms of electrostatic force, which is the major factor of the particle dispersion in the electrostatic precipitator. The model was validated by comparing the calculated data with the experimental measurements. Within the scope of this research, the following conclusions can be made:

(1) For ultrafine particles, the drift flux caused by the momentum change rate per unit volume of particle phase (D) and the drift flux caused by the momentum transport by the particle fluctuation due to turbulence (S_{mp}) have little effect on particle distribution.
(2) For particles with a diameter in the range of 0.01 to 0.1 μm, the thermophoresis force may be larger than the gravitational force, but both forces are relatively too small to affect the particle distribution.
(3) In the zone below 1 meter, concentrations of ultrafine particles in a room with a mixing ventilation mode are higher than those in a room with displacement ventilation, which is different than for micron particles.

(4) Both ventilation modes studied herein are not sensitive to the particle size when the diameters are in the range from 0.01 to 0.1 μm.
(5) The concentration distributions of ultrafine particles in mixing ventilation are more symmetrical than those in displacement ventilation.

Acknowledgments

The authors would like to acknowledge the financial support from the National Key Technology R&D Program (no. 2006BAJ02A10), China, and the assistance in experimental data collection by Mr. Yiming Ji of the University of Calgary.

References

Chen, F., Yu, S. C. M., & Lai, A. C. K. (2006). Modeling particle distribution and deposition in indoor environments with a new drift-flux model. *Atmospheric Environment*, *40*, 357–367.
Elghobashi, S. (1994). On predicting particle-laden turbulent flows. *Applied Scientific Research*, *52*, 309–329.
EPA (2005). Review of the national ambient air quality standards for particulate matter: Policy assessment of scientific and technical information, OAQPS Staff Paper.
Ferin, J., Oberdoerster, G., Penney, D. P., Soderholm, S. C., Gelein, R., & Piper, H. C. (1990). Increased pulmonary toxicity of ultrafine particles? 1. Particle clearance, translocation, morphology. *Journal of Aerosol Science*, *21*, 381–384.
Gao, N., & Niu, J. (2007). Modeling particle dispersion and deposition in indoor environments. *Atmospheric Environment*, *41*, 3862–3876.
Golshahi, L. (2007). Experimental and modeling studies of granular filtration for airborne particles. Master of Science Thesis, University of Calgary, Canada.
He, G. (2003). Modeling indoor pollutant exposures under different ventilation schemes. Ph.D. Dissertation, Department of Civil, Architectural, and Environmental Engineering, University of Miami, Coral Gables, FL, USA.
Hinds, W. C. (1999). *Aerosol technology: Properties, behavior, and measurement of airborne particles*. 2nd ed., New York: Wiley.
Hinze, J. O. (1975). *Turbulence*, 2nd ed., New York: McGraw-Hill.
Holmberg, S., & Chen, Q. (2003). Air flow and particle control with different ventilation systems in a classroom. *Indoor Air*, *13*, 200–204.
Holmberg, S., & Li, Y. (1998). Modelling of the indoor environment—particle dispersion and deposition. *Indoor Air*, *8*, 113–122.
Kittelson, D. B. (1998). Engines and nanoparticles: A review. *Journal of Aerosol Science*, *29*, 575–588.
Liu, X., & Zhai, Z. (2007). Identification of appropriate CFD models for simulating aerosol particle and droplet indoor transport. *Indoor and Built Environment*, *16*, 322–330.
Murakami, S., Kato, S., Nagano, S., & Tanaka, S. (1992). Diffusion characteristics of airborne particles with gravitational settling in a convection-dominant indoor flow field. *ASHRAE Transactions*, *98*, 82–97.
Talbot, L., Cheng, R. K., & Schefer, R. W. (1980). Thermophoresis of particles in a heated boundary layer. *Journal of Fluid Mechanics*, *101*(4), 737–758.
Zhao, B., Li, X., & Yan, Q. (2003). A simplified system for indoor airflow simulation. *Building and Environment*, *38*, 543–552.
Zhao, B., Li, X., & Zhang, Z. (2004). Numerical study of particle deposition in two different kind of ventilated rooms. *Indoor and Built Environment*, *13*, 443–451.
Zhao, B., Zhang, Y., Li, X., Yang, X., & Huang, D. (2004). Comparison of indoor aerosol particle concentration and deposition in different ventilated rooms by numerical method. *Building and Environment*, *39*, 1–8.
Zhou, L. (1993). *Theory and modeling of turbulent gas–particle flows and combustion*. Beijing: Science and CRC Press.